Removal of organic contaminant by municipal sewage sludge-derived hydrochar: kinetics, thermodynamics and mechanisms

Jia Wei, Yitao Liu, Jun Li, Hui Yu and Yongzhen Peng

ABSTRACT

In this work, a microporous municipal sewage sludge-derived hydrochar (MSSH) with relatively high surface area and abundant surface organic functional groups was produced through hydrothermal carbonization. Based on the adsorption results over a wide range of conditions, the prepared MSSH was suggested as a promising adsorbent for CV because of its high and efficient adsorption capability. The experimental data were fitted to several kinetic models. Based on calculated respective parameters such as rate constants, equilibrium adsorption capacities and correlation coefficients, the pseudo second-order model proved the best in describing the adsorption behavior of MSSH. Through kinetics, thermodynamic modeling studies and material characterization, a plausible adsorption process was discussed under the conditions used in this study. It can be confirmed that the adsorption of CV onto MSSH is via both physical interactions (electrostatic interaction and Van der Waals' force) and chemical interactions (formation of H-bonding).

Key words | adsorption, crystal violet, hydrochar, hydrothermal carbonization, municipal sewage sludge

Jia Wei (corresponding author)
Yitao Liu
Jun Li
College of Architecture Engineering,
Beijing University of Technology,
100 Pingleyuan, Chaoyang district,
Beijing, 100124,
China
E-mail: *weij@bjut.edu.cn*

Hui Yu
College of Civil and Environmental Engineering,
Temple University,
1947 N.12th Street, Philadelphia, PA 19122,
USA

Yongzhen Peng
National Engineering Laboratory for Advanced Municipal Wastewater Treatment and Reuse Technology, Engineering Research Center of Beijing,
Beijing University of Technology,
Beijing, 100124,
China

INTRODUCTION

In recent years, with the rapid development of urban construction in China, the quality of effluent treatment standards has improved to be more stringent, which has resulted in drastically increasing production of sewage sludge, from 9 million metric tonnes in 2005 (He *et al.* 2007) to 34 million metric tonnes in 2015 (Feng *et al.* 2015) (at a moisture content of 80%). Sewage sludge is of crucial concern because it can contribute to secondary pollution in the soil and aquatic environment if it is not properly disposed of. Most of the sludge has been disposed of by conventional ways including composting, land/ocean disposal and incineration, and so on. Moreover, these methods are gradually being limited by the rigorous requirements of environmental protection. Currently, less than 30% of the sewage sludge in China has been treated safely (Zhen *et al.* 2014). Some new recycling technologies for disposal of sewage sludge like anaerobic digestion/aerobic composting and biomass recycling (Boixa *et al.* 2016) are being widely advocated at present. Nevertheless, the output from sludge treatment by anaerobic digestion or aerobic composting is inferior because of the low organic matter content. Biomass recycling is a promising technology for the treatment of sludge embracing biomass gasification, liquefaction and carbonization. Thereunto, biomass gasification and liquefaction are greatly endothermic and require high temperature usually in the range of 700–1,200 °C (gasification) (Peterson *et al.* 2008) and 300–550 °C (liquefaction) (Yuan *et al.* 2015). Latterly, biomass carbonization has been deemed as a promising technology for the synthesis of novel carbon derived materials with a wide variety of potential applications.

Biochar is the solid product of biomass carbonization, which is defined as a 'solid substance obtained by thermochemical conversion of biomass in oxygen-limited environments' by the International Bioconcentration Organization (IBI) (Initiative 2012). Biochar is capable of being made from crops, poultry droppings and sewage sludge through pyrolysis or hydrothermal carbonization (HTC) methods (Cha *et al.* 2016). Pyrolysis typically utilizes dry biomass for the production of biochar. However, most biomass materials have high moisture contents and thus a separate

doi: 10.2166/wst.2018.373

drying step is required to obtain high product yields which reduces the process energy. The hydrothermal process takes place at low temperatures under autogeneous pressures in aqueous media, which is anticipated to be able to remedy the shortcoming of dry processes (Song *et al.* 2017). The products obtained by the hydrothermal method are also called hydrochar. For instance, coconut fiber and dead eucalyptus leaves with high moisture content was hydrothermally carbonized at 150–375 °C for 0.5 h and high heating value products were obtained (Liu *et al.* 2013). Hydrochar derived from macroalgae (180–210 °C) by Xu *et al.* (Xu *et al.* 2013) possessed carbon contents of 36.8–50.5% and high heating values of 19.0–25.1 $MJ{\cdot}kg^{-1}$. Because of its high energy efficiency and potential soil quality benefits, hydrochar has attracted significant attention as a fuel and soil amendment. In addition, the sorption of contaminants from water onto hydrochar is advantageous in terms of its high surface area, microporosity, chemical stability, convenience and economy. Pine needles were converted into hydrochar via HTC at 225 °C (Hammud *et al.* 2015) and applied to Malachite Green removal. The adsorption capacity of pine needle hydrochar reached 52.91 $mg{\cdot}g^{-1}$. A typical agricultural biomass waste, rice husk, was pretreated using simple HTC technology (170–280 °C) by Ding *et al.* and the prepared hydrochar was used for hexavalent chromium (Cr(VI)) removal from aqueous solutions. The results showed that the novel HTC pretreated rice husk hydrochar was a prospective adsorbent for Cr(VI) removal (Ding *et al.* 2016).

Dyes are common organic contaminants arising from various industries such as textiles, leather, paper, plastics and printing (Puchana-Rosero *et al.* 2017). The presence of dyes in water bodies not only affects their aesthetic nature but also reduces light penetration and effects on the photosynthetic phenomenon for aquatic life (Vakili *et al.* 2014). In up-to-date data, more than 100,000 commercial dyes are known with an annual production of over 7×10^5 tonnes/year globally (Sen *et al.* 2011). So far, many conventional methods have been utilized to remove dyes from wastewater, such as adsorption on various sorbents (Mavinkattimath *et al.* 2017), chemical decomposition by oxidation (Alshamsi *et al.* 2014), photodegradation (Lu *et al.* 2017) and microbiological (Daneshvar *et al.* 2007). Nevertheless, chemical and biological methods are arduous, since dyes are resistant to aerobic digestion and are stable to light and oxidizing agents (Srivastava *et al.* 1997). Additionally, several organic and inorganic adsorbents have been tested for the removal of organic dyes from wastewaters, such as activated carbon (Dabrowski *et al.* 2005) and carbon graphitic nanostructures (Lu *et al.* 2006). Although some of them have indicated a rather superior removal performance, there are certain limitations in their practical applications on account of high manufacturing cost and strict preparation conditions (Cao *et al.* 2014).

In this context, a proper adsorbent for dye pollution is a compulsory challenge that appears to have essential financial and environmental burdens. Plant derived hydrochar has been investigated extensively in the aforementioned studies. However, sewage sludge has the characteristic of high moisture content and poor dewaterability which can be stabilized and sanitized by HTC. Furthermore, there are few reports on municipal sewage sludge-derived hydrochar (MSSH), especially as an emerging adsorbent. In this study, the sewage sludge was used as a raw material to prepare an absorbent by HTC. The adsorption kinetics and thermodynamics were utilized to investigate the adsorption process for crystal violet (CV). The corresponding features of MSSH were also characterized by various techniques, which can assist in exploring the adsorption process. The results from this study will offer an effective way of treating sludge, present a preparation method for a high efficiency adsorbent and provide a realistic estimate for the environmental behavior of an organic pollutant in contaminated water.

MATERIALS AND METHODS

Materials

The sewage sludge (moisture content 99.6%, pH 6.7), taken from the Gaobeidian sewage treatment plant in China, was used as a carbon source for the production of hydrochar. The organic contaminant was CV ($C_{25}H_{30}IN_3$, 407.99 $g{\cdot}mol^{-1}$, purity ≥99%) obtained from Tianjin Institute of Refractories and Fine Chemicals. The stock solution of contaminant (used as purchased without further purification) with a concentration of 1,000 $mg{\cdot}L^{-1}$ was diluted to the desired concentration. The solution pH was adjusted using 0.1 M HCl or 0.1 M NaOH solution. All solutions were prepared using high purity deionized water with an electrical conductivity of 2 $\mu S{\cdot}cm^{-1}$.

Preparation of municipal sewage sludge-derived hydrochar

A certain amount of sewage sludge was placed into an electric blast oven and dried to constant weight at 105 °C. Then the dried sludge was ground into fine powder (<250 μm) for subsequent HTC experiments, which were conducted in a

1 L high pressure autoclave equipped with stirrer bar, heater coil, temperature control, water cooling coil and venting valve for gases. The preliminary experiment proved that a hydrothermal temperature of 180 °C, retention time of 3 h and sludge powder: deionized water = 1:9 (weight ratio) were the optimum preparation conditions. The obtained product was separated by centrifugation at 5,000 rpm for 10 min and rinsed several times with distilled water to wipe off the surface residue. Afterwards, it was transferred to a drying oven set at 105 °C for 24 h and passed through a 70 mesh nylon sieve. Finally, the fraction containing particles with a size <210 μm was sealed in plastic bags in the dark and stored in a desiccator at a room temperature.

Material characterization

The surface morphological characteristics of both the raw sludge and obtained MSSH were observed by scanning electron microscopy (SEM) (Model JSM-7401, Nippon Electronics). Fourier transform infrared spectra (FTIR) were recorded on a Nicolet 6,700 (Thermo, USA) spectrometer, and the spectra were scanned over the range of 400–4,000 cm^{-1}. Moreover, the specific surface area and pore size of MSSH were calculated from N_2 sorption isotherms by the Brunauer-Emmett-Teller (BET) method. (The sample was degassed at 105 °C for 24 h and the liquid nitrogen temperature was 77 K). In addition, the surface charge situation at the varying pH of hydrochar was measured by Zeta potentiometer (Zetasizer Nano ZS, UK).

Adsorption experiment

Typically, the roles of adsorbent dosage, pH and initial contaminant concentrations were considered crucial in the adsorption process. In duplicate batch experiments, 40 mL standard sample vials with Teflon-lined septa and screw caps were utilized. The above experiments were conducted in a constant temperature shaker (air bath). The preliminary experiment has proved that 24 h reaction time is sufficient to ensure contact between adsorbate and adsorbent. Then, solutions were centrifuged for 20 min in the centrifuge at a 5,000 rpm rotation speed. A small amount of supernatant was taken out after centrifugation and diluted to a certain multiple. The organic pollutant concentration was determined eventually by a 765 UV-vis spectrophotometer with the absorbance measured at $\lambda = 580$ nm in curettes.

The influence factors experiments were performed under the following conditions: During the adsorption experiments, five changes in the adsorbent dose from 2 to 10 $g{\cdot}L^{-1}$ were made to investigate the influence of MSSH dosage on CV adsorption. In the study of the pH effect, pH was tested across the range of 2–12. The effect of initial CV concentrations was investigated by adding a certain amount of adsorbent to different concentrations (50–350 $mg{\cdot}L^{-1}$) of CV solution.

The thermodynamics experiments proceeded at 10, 20, and 30 °C respectively using 6 $g{\cdot}L^{-1}$ of MSSH in 25 mL CV solution with different initial concentrations for 24 h. The experimental data was applied to calculate the thermodynamic parameters.

Adsorption kinetics experiments were conducted at 30 °C and an initial CV concentration of 250 $mg{\cdot}L^{-1}$. The solution was shaken at 200 rpm in an air bath shaker and the CV concentrations at different time intervals were determined until equilibration.

The adsorption rate is calculated by formula (1):

$$Adsorption\,rate = \frac{(C_0 - C_e)}{C_0} \times 100\% \quad (1)$$

where C_0 and C_e are the initial and final concentrations of CV ($mg{\cdot}L^{-1}$).

The adsorption capacity of CV on the adsorbent is calculated as (2):

$$Q_t = \frac{V(C_0 - C_t)}{m} \quad (2)$$

where V (L) is the solution volume; C_0 ($mg{\cdot}L^{-1}$) and C_t ($mg{\cdot}L^{-1}$) denote the concentrations of CV at the start and at time t, respectively; m (g) is the adsorbent mass; Q_t ($mg{\cdot}g^{-1}$) is the amount of CV adsorbed on the adsorbent at time t.

RESULTS AND DISCUSSION

Characteristics of MSSH

The images on the surface morphology of raw sludge and MSSH are shown in Figure 1. The surface of the raw sludge is dense and planar without any pores and crevices. In contrast, there are plentiful loose flocculates over the surface of the MSSH, forming an advanced pore network system. The porosity of the adsorbent is very important in the adsorption process, which leads to the increase of the surface area and adsorption capacity. The concave and convex parts of MSSH are uneven and very rough. It can

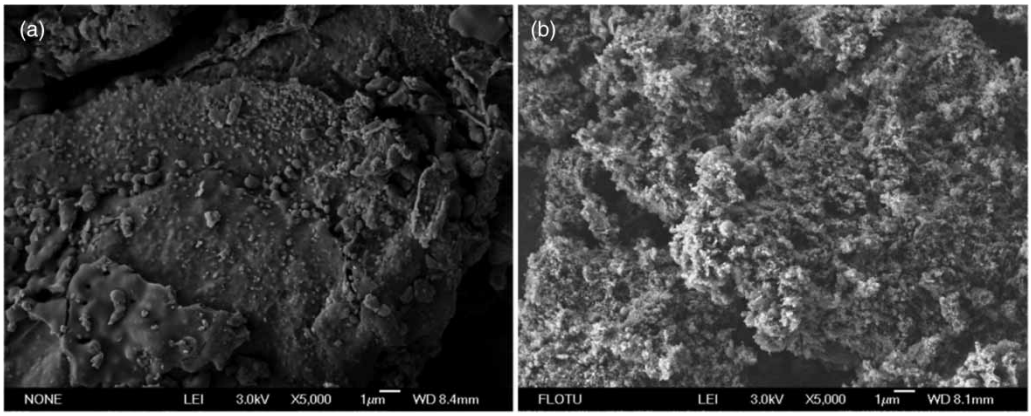

Figure 1 | SEM micrograph of raw sludge (a) and MSSH (b). (Images with 5,000 magnification).

be ensured that the pores of products are increased greatly through hydrothermal carbonation.

The results of BET (Table 1) manifest the surface area and pore volume of MSSH, which are 9.1-fold and 21.9-fold greater than that of raw sludge, respectively. At the same time, the average pore diameter of a sample decreases after HTC. It can be confirmed that the MSSH contains micropores mainly by calculating the average pore diameter (1.425 nm).

FTIR analysis (Figure 2) presents typical structural properties of MSSH. The peak at 1,080 cm^{-1} appears in both of the FTIR spectra, which is characteristic of the -OH groups. The peaks at 1,460 cm^{-1} and 1,642 cm^{-1} are assigned to C = C bonds in aromatic compounds and carboxylate groups, respectively. The band at 2,922 cm^{-1} corresponds to −COOH stretching vibration. The −OH stretching of the free −COOH is between 3,250 and 3,600 cm^{-1}. Peak height and band area in a FTIR spectrum are widely used to indicate the concentration of a certain bond. The results show that organic functional groups still remain on the surface of MSSH and are even enhanced in number compared with raw sludge. The large number of oxygen-containing functional groups may facilitate the chemical adsorption.

Table 1 | Pore size information of the samples

Hydrochar samples	Surface area ($m^2 \cdot g^{-1}$)	Pore volume ($cc \cdot g^{-1}$)	Average pore diameter (nm)
Raw sludge	4.966	0.015	3.074
MSSH	45.282	0.382	1.425

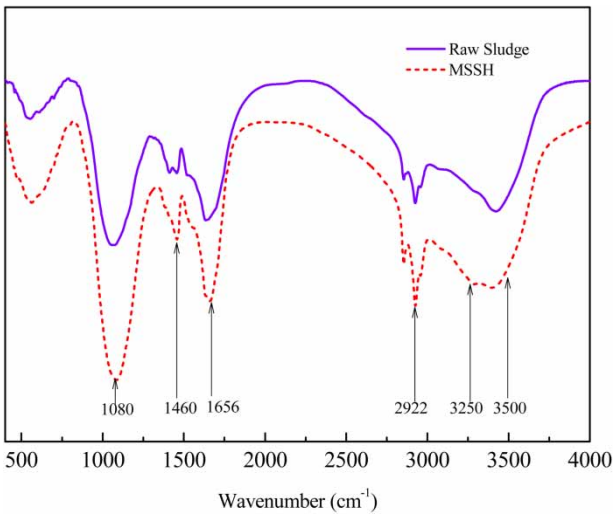

Figure 2 | FTIR images of raw sludge and MSSH.

Adsorption of CV on MSSH

Effect of MSSH dosage

Figure 3(a) illustrates that by adding adsorbent dosage from 2 to 6 $g \cdot L^{-1}$, the CV adsorption rate sharply increases from 93.94% to 99.01%. Further increasing the adsorbent dosage to 8 $g \cdot L^{-1}$, the adsorption rate drops slightly. This may be owing to the collision of MSSH particles with each other leading to the separation of absorbed CV molecules. It is also possible that the MSSH particles are aggregated with each other as the dosing amount is excessive, resulting in a decrease of the specific surface area that hinders the entry of the CV molecules into the MSSH. Herein, the optimum dosage for the removal of CV by MSSH is found to be 6 $g \cdot L^{-1}$.

Effect of pH value

pH is a key factor that influences the adsorption of CV on the surface of an adsorbent (Kumar *et al.* 2014). As displayed in

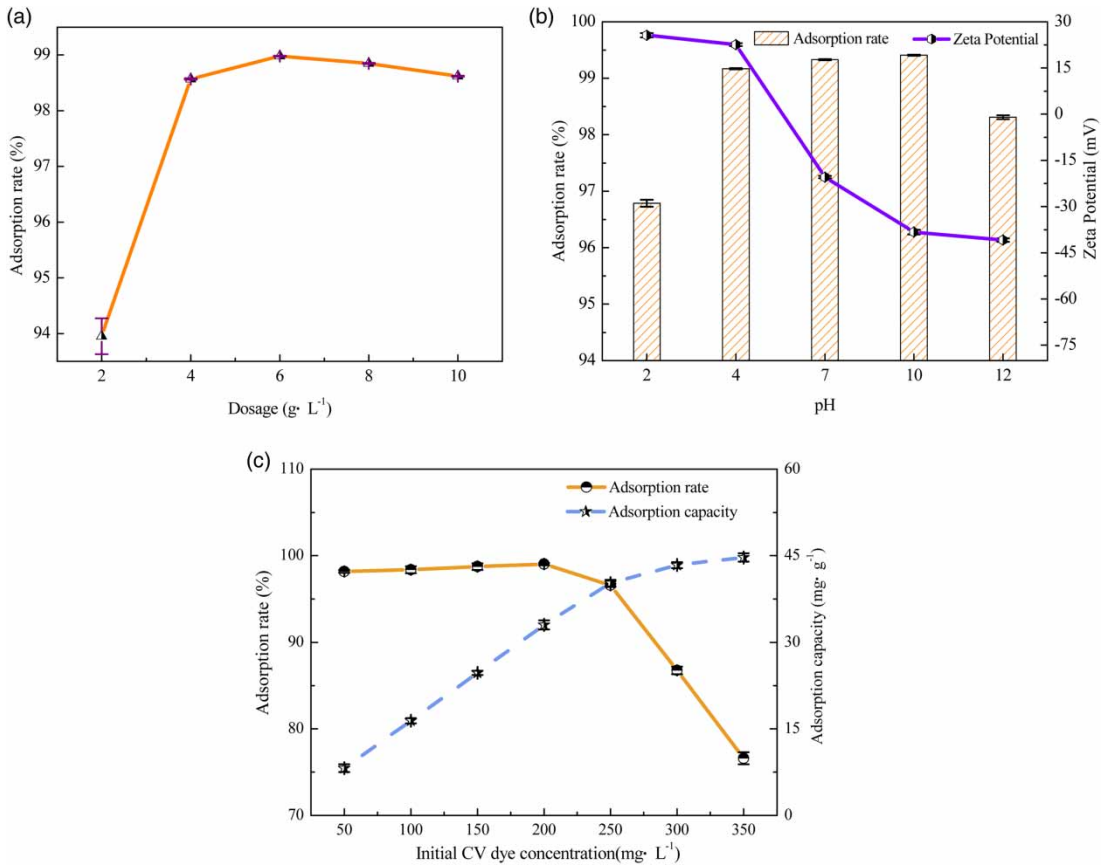

Figure 3 | Adsorption performance of MSSH in different conditions. (a) Adsorbent dosage (initial CV concentration, 150 mg·L^{-1}, 20 °C); (b) initial solution pH (initial CV concentration, 150 mg·L^{-1}, 20 °C and dosage is 6 g·L^{-1}); (c) initial CV concentration (dosage, 6 g·L^{-1}, 20 °C).

Figure 3(b), the adsorption rate increases with the pH value and reaches the maximum at pH = 10. According to the zata potential of MSSH, the surface of MSSH is positively charged under acidic conditions. When pH reaches to 7 or is greater than 7, the surface of MSSH becomes negatively charged. Meanwhile, the molecules of CV contain tertiary amine groups and are cationic in acidic media, while present as neutral and nonionic in strong alkaline solutions. Here, MSSH expresses low adsorption capacity as pH < 4, which is ascribed to the electrostatic repulsion between MSSH and CV. As the pH value is between 7 to 10, the electrostatic interaction enhances the adsorption, which is due to the opposite potentials of MSSH and CV. Furthermore, the number of protonated cationic group of CV has an electrostatic interaction with adsorbent and declines as pH at a high level (pH = 12), bringing about diminished CV adsorption.

Effect of initial CV concentrations

In the low concentration range, the removal percentage and adsorption amount of CV are growing slightly with an increase in the initial CV concentration (Figure 3(c)), which provides an improvement in driving force for the combination of the CV and the adsorption sites. As the concentration of CV exceeds 250 mg·L^{-1}, the adsorption rate begins to decline sharply and the adsorption capacity tends to be stable. On one hand, the solution contains a large number of CV molecules, which not only increase the probability of collision with the adsorption site, but also raise the exclusion between the molecules. The exclusion is unfavorable to the combination of CV molecules and adsorption site. On the other hand, the MSSH combines substantial crystal molecules which occupy the adsorption sites on MSSH by CV completely, hence preventing further integration of MSSH and CV.

Thermodynamic analysis

For better understanding the adsorption of CV on MSSH, three thermodynamic parameters, ΔH, ΔS and ΔG are investigated respectively. The thermodynamic parameters are determined by the Van't Hoff equation

(Equation (3)).

$$\ln K_d = -\frac{\Delta G}{RT} = -\frac{\Delta H}{RT} + \frac{\Delta S}{R} \quad (3)$$

where R is the gas constant (8.314 J·(mol·K)$^{-1}$); T is the kelvin temperature (K); K_d is the equilibrium constant, and the formula is as follows:

$$K_d = q_e/C_e \quad (4)$$

where q_e (mg·g^{-1}) is the amount of adsorbed CV in unit mass of MSSH; C_e (mg·L^{-1}) is the concentration of CV in adsorption equilibrium.

The thermodynamic parameters ΔH and ΔS are calculated from the slope and intercept of the Van't Hoff plots of lnK_d versus $1/T$ (Figure 4) and the results are shown in Table 2. The positive ΔS values (129.03–184.82 J·(mol·K)$^{-1}$) suggest a magnification in the degrees of randomness at the interface between the solid and liquid during the adsorption process (Liu *et al.* 2010). The adsorption and desorption usually co-exist in the adsorption reaction. In the case of CV molecules absorbed on MSSH, there exists multiple water molecules desorption. The molecular weight of CV is greater than water, which brings about increased entropy of the whole system.

The positive values of ΔH demonstrate that the adsorption process is endothermic. The elevated temperature is favorable to the forward progress of the reaction and the improvement of the adsorption rate. As the initial concentration increases, the presence of ΔH >40 kJ·mol^{-1} elucidates that chemical adsorption starts to appear in the process of CV adsorption on MSSH (Alkan *et al.* 2004). Based on the thermodynamic calculation and the preceding material characterization, a plausible chemical adsorption process can be inferred, that the N atom of CV could form H-bonding with the H atom of the oxygen-containing functional groups (such as the carboxyl group and hydroxyl group) on the adsorbent surface. In order to complete the discussion, Figure 5 graphically illustrates the H-bonding mechanism for CV adsorption on the MSSH.

The Gibbs free energy change ΔG can be calculated by the following equation:

$$\Delta G = \Delta H - T\Delta S \quad (5)$$

With the change of temperature and initial concentration, the values of ΔG (Table 2) are all negative, supporting the adsorption reaction being a spontaneous process. It is noted that the values of ΔG up to −20 kJ·mol^{-1} are consistent with electrostatic interaction between sorption sites and adsorbate (physical adsorption) (El-Etre 2007; Jordão *et al.* 2009). The ΔG values obtained in this study confirm the adsorption spontaneity and feasibility of MSSH, as well as physical adsorption having the predominant role in the sorption process.

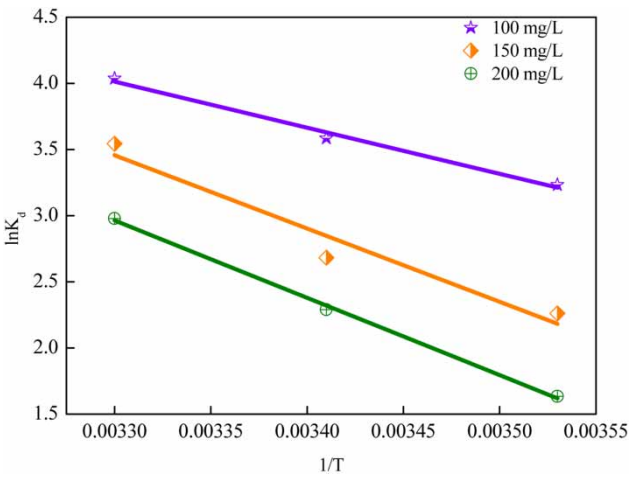

Figure 4 | Van't Hoff plot.

Adsorption kinetics

To gain insight into the adsorption process of CV on MSSH, several adsorption kinetic models were selected to determine the relationship between the amount of adsorbate

Table 2 | Thermodynamic parameters

			ΔG (kJ·mol^{-1})			$T\Delta S$ (kJ·mol^{-1})		
C_0 (g·L^{-1})	ΔH (kJ·mol^{-1})	ΔS (J·(mol·K)$^{-1}$)	283.15 K	293.15 K	303.15 K	283.15 K	293.15 K	303.15 K
100	29.00	129.03	−7.54	−8.83	−10.12	36.54	37.83	39.12
150	46.08	180.66	−5.07	−6.88	−8.68	51.15	52.96	54.77
200	48.54	184.82	−3.79	−5.64	−7.49	52.33	54.18	56.03

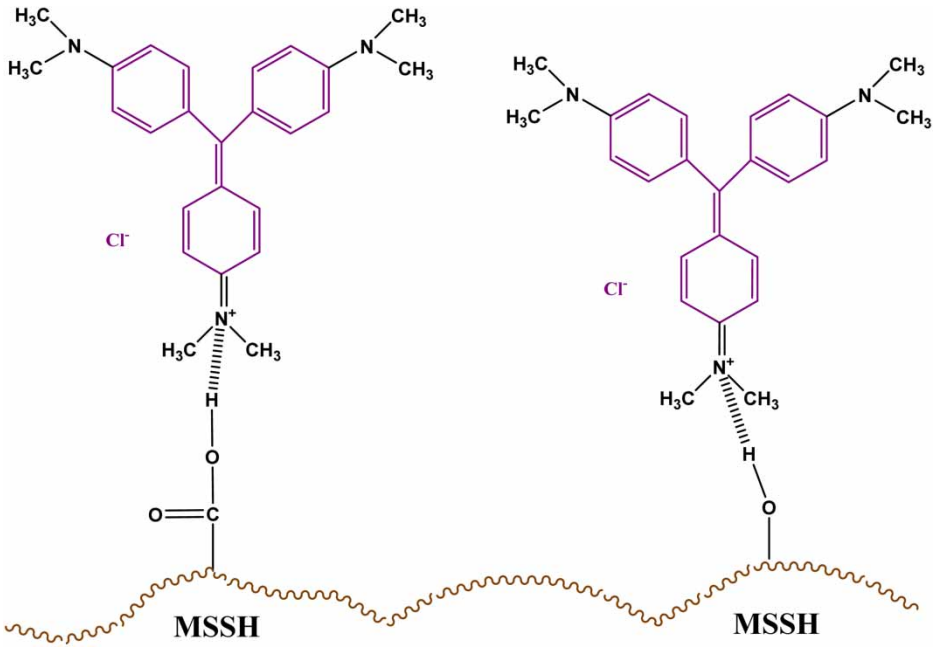

Figure 5 | Schematic of chemisorption of CV and MSSH.

and reaction time, as well as to fit the experimental data obtained under the optimal laboratory conditions.

Both the pseudo-first order kinetic model (Figure 6(a)) and pseudo-second order kinetic model (Figure 6(b)) are exploited in this study. In order to separate different diffusion stages during the adsorption, the role of diffusion in the speed of the adsorption can be further examined, adopting the so called intra-particle diffusion model (Figure 6(c)). Three kinetic models are summarized in Table 3.

The results manifested that the correlation coefficient R^2 of the pseudo-second order kinetic model is 0.9997, which is higher than that of the pseudo-first order kinetic model. Therefore, it is considered that the pseudo-second order kinetic model accurately describes the adsorption process of CV on the MSSH. This also indicates that chemical sorption is the rate-limiting step, which involves the formation of H-bonding between the N atom of CV and the H atom of the oxygen-containing functional groups on the MSSH surface (Ho & Mckay 1999). But at the same time, the initial rapid phase within the first 180 minutes may involve physical adsorption on the surface of hydrochar. Therefore, there are at least two mechanisms involved in the actual process. Similar results were also observed in the adsorption of malachite green onto hydrochar derived from phycocyanin-extracted algal bloom residues (Zhang *et al.* 2017).

From the plots of q_t versus $t^{1/2}$ of CV (Figure 6(c)), a multi-linearity is observed, denoting a three step adsorption process. The first step, the sharp portion, is attributed to film diffusion (diffusion of the CV through the solution to the external surface of the MSSH, or the boundary layer diffusion of CV molecules). The second region relates to diffusion in the liquid contained in the pores, where intra-particle diffusion is the rate limiting step. In the final equilibrium step, the intra-particle diffusion starts to decrease because of the low CV concentration left in the solution. The plot does not pass through the origin, demonstrating that intra-particle diffusion is not the only rate controlling step. Presumably, film diffusion or chemical reaction controls the adsorption rate (Tian *et al.* 2014). The parameter B represents the thickness of the boundary layer. As displayed in Table 3, the values of B increase in the first 180 minutes and are constant during 180–1,800 min. This proves that the influence of the boundary layer increases with time at first and then achieves stability.

In this regard, the adsorption process may be jointly controlled by pore diffusion, surface adsorption and intra-particle diffusion. In the first stage, the membrane diffusion rate is very fast. As the adsorption surface of the adsorbent is saturated, the CV gradually enters the internal voids of the MSSH. During the diffusion progresses, the diffusion resistance gradually increases and finally reaches the adsorption equilibrium.

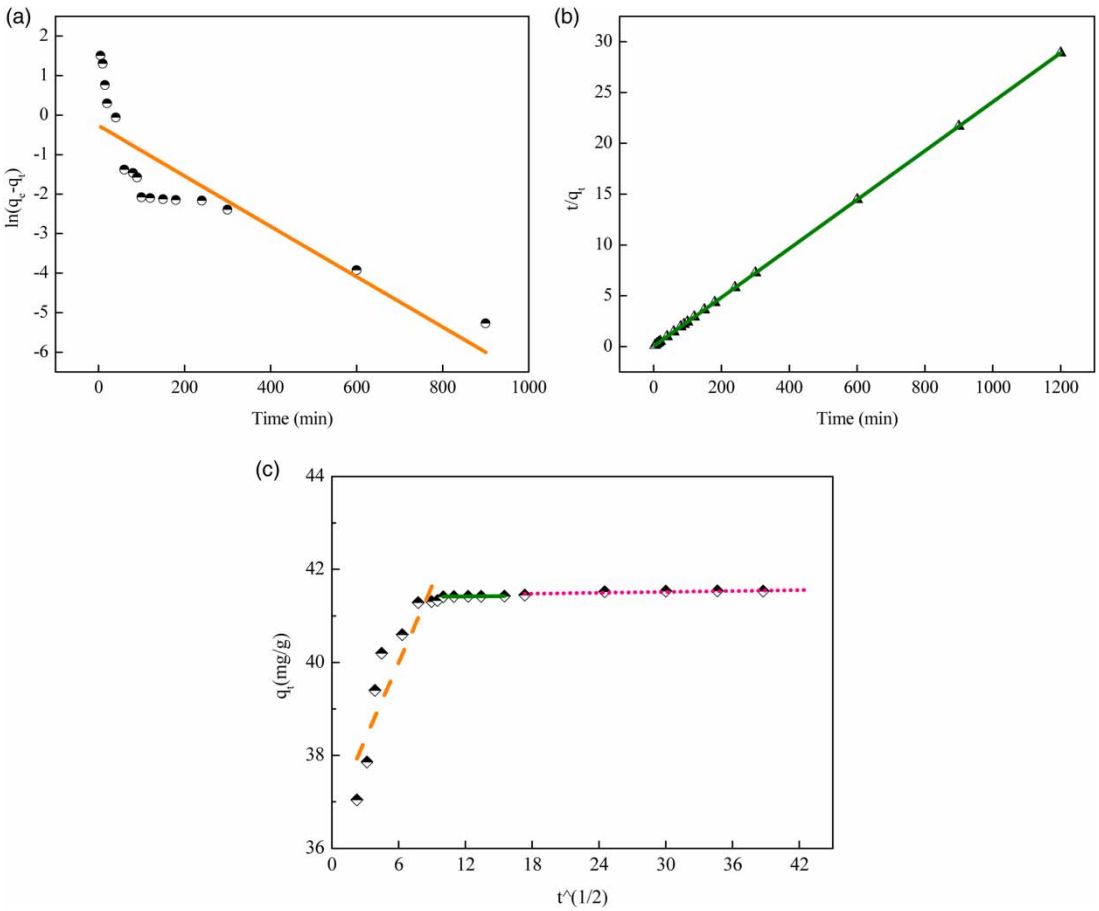

Figure 6 | Adsorption kinetic models. (a) Pseudo-first order kinetic; (b) pseudo-second order kinetic; (c) intra-particle diffusion kinetic.

Table 3 | Kinetic models and fitting parameters

Models	Equation	$K_1 \times 10^3$	R^2		
Pseudo-first order kinetic	$\ln(q_e - q_t) = \ln q_e - k_1 t$	6		0.719	
Pseudo-second order kinetic	$t/q_t = 1/k_2 q_e^2 + t/q_e$	$K_2 \times 10^3$		R^2	
		41.142		0.9997	
Intra-particle diffusion kinetic	$q_t = K_p t^{1/2} + B$	Time (min)	K_p	B	R^2
		0–100	0.54907	36.70357	0.80170
		100–180	0.00318	41.39573	0.93953
		180–1,800	0.00190	41.41946	0.61598

CONCLUSIONS

In this research a sewage sludge derived hydrochar was successfully synthesized by HTC under benign conditions. The prepared MSSH has a relatively high surface area, well developed porosity and abundant surface organic functional groups, which were beneficial for contaminant removal. Optimum values of experimental parameters were investigated and it can be confirmed that the electrostatic interaction had a key role in the adsorption process. Moreover, the successful fitting of pseudo-second order models suggested that the chemical interaction (which can form H-bonding between the N atom of CV and H atom of the oxygen-containing functional groups on the MSSH surface) was the rate-controlling step in the adsorption process.

ACKNOWLEDGEMENTS

Authors would like to acknowledge the financial support by the National Natural Science Foundation of China (51778015), China Postdoctoral Science Foundation (2016M600886) and Beijing Postdoctoral Science Foundation (2016ZZ-31).

REFERENCES

Alkan, M., Demirbaş, Ö., Çelikçapa, S. & Doğan, M. 2004 Sorption of acid red 57 from aqueous solution onto sepiolite. *J. Hazard. Mater.* **116** (1–2), 135–145.

Alshamsi, H., Adilee, K. J. A. & Jaber, S. A. 2014 Synthesis, characterization, thermal and kinetic photo chemical decomposition study of new azo dye 7-[2-(BenzImidazolyl) Azo]-8-Hydroxy quinoline and its znic (II) complex. *Chem. Mater. Res.* **6** (8), 69–80.

Boixa, C., Ibáñeza, M., Fabregat-Safonta, D., Moralesb, E. & Pastorb, L. 2016 Behaviour of emerging contaminants in sewage sludge after anaerobic digestion. *Chemosphere* **163**, 296–304.

Cao, J., Lin, J., Fang, F., Zhang, M. & Hu, Z. 2014 A new absorbent by modifying walnut shell for the removal of anionic dye: kinetic and thermodynamic studies. *Bioresource Technol.* **163** (7), 199–205.

Cha, J. S., Park, S. H., Jung, S. C., Ryu, C., Jeon, J. K., Shin, M. C. & Park, Y. K. 2016 Production and utilization of biochar: a review. *J. Ind. Eng. Chem.* **40**, 1–5.

Dabrowski, A., Podkościelny, P., Hubicki, Z. & Barczak, M. 2005 Adsorption of phenolic compounds by activated carbon-a critical review. *Chemosphere* **58** (8), 1049–1070.

Daneshvar, N., Ayazloo, M., Khataee, A. & Pourhassan, M. 2007 Biological decolorization of dye solution containing Malachite Green by microalgae *Cosmarium* sp. *Bioresource Technol.* **98** (6), 1176–1182.

Ding, D., Ma, X., Shi, W., Lei, Z. & Zhang, Z. 2016 Insights into mechanisms of hexavalent chromium removal from aqueous solution by using rice husk pretreated using hydrothermal carbonization technology. *RSC Adv.* **6**, 74675–74682.

El-Etre, A. Y. 2007 Inhibition of acid corrosion of carbon steel using aqueous extract of olive leaves. *J. Colloid Interface Sci.* **314** (2), 578–583.

Feng, L., Jing, Y. L. & Chen, Y. 2015 Dilemma of sewage sludge treatment and disposal in China. *Environ. Sci. Technol.* **49** (8), 4781–4782.

Hammud, H. H., Shmait, A. & Hourani, N. 2015 Removal of Malachite Green from water using hydrothermally carbonized pine needles. *RSC Adv.* **5**, 7909–7920.

He, P., Lü, F., Zhang, H., Shao, L. & Lee, D. 2007 Sewage sludge in China: challenges toward a sustainable future. *Water Pract. Technol.* **2**, 19–22.

Ho, Y. & Mckay, G. 1999 Pseudo-second order model for sorption processes. *Process Biochem.* **34** (5), 451–465.

Initiative, I. B. 2012 *Standardized Product Definition and Product Testing Guidelines for Biochar That is Used in Soil*. International Biochar Initiative.

Jordão, C. P., Fernandes, R. B. A., Ribeiro, K. L., Nascimento, B. S. & Barros, P. M. 2009 Zn(II) adsorption from synthetic solution and kaolin wastewater onto vermicompost. *J. Hazard. Mater.* **162** (2–3), 804–811.

Kumar, V. V., Sivanesan, S. & Cabana, H. 2014 Magnetic cross-linked laccase aggregates-bioremediation tool for decolorization of distinct classes of recalcitrant dyes. *Sci. Total Environ.* **487** (1), 830–839.

Liu, Q., Zheng, T., Wang, P., Jiang, J. & Li, N. 2010 Adsorption isotherm, kinetic and mechanism studies of some substituted phenols on activated carbon fibers. *Chem. Eng. J.* **157** (2–3), 348–356.

Liu, Z., Quek, A., Hoekman, S. K. & Balasubramanian, R. 2013 Production of solid biochar fuel from waste biomass by hydrothermal carbonization. *Fuel* **103** (1), 943–949.

Lu, A., Li, W., Salabas, E. L., Spliethoff, B. & Schüth, F. 2006 Low temperature catalytic pyrolysis for the synthesis of high surface area, nanostructured graphitic carbon. *Chem. Mater.* **18** (8), 2086–2094.

Lu, N., Yeh, Y. P., Wang, G. B., Feng, T. Y., Shih, Y. H. & Chen, D. 2017 Dye-sensitized TiO_2-catalyzed photodegradation of sulfamethoxazole under blue or yellow light. *Environ. Sci. Pollut. Res.* **24** (1), 489–499.

Mavinkattimath, R. G., Kodialbail, V. S. & Govindan, S. 2017 Simultaneous adsorption of Remazol brilliant blue and Disperse orange dyes on red mud and isotherms for the mixed dye system. *Environ. Sci. Pollut. Res.* **24** (23), 18912–18925.

Peterson, A. A., Vogel, F., Lachance, R. P., Fröling, M. & Tester, J. W. 2008 Thermochemical biofuel production in hydrothermal media: a review of sub- and supercritical water technologies. *Energ. Environ. Sci.* **1** (1), 32–65.

Puchana-Rosero, M. J., Lima, E. C., Ortiz-Monsalve, S., Mella, B., Costa, D., Poll, E. & Gutterres, M. 2017 Fungal biomass as biosorbent for the removal of Acid Blue 161 dye in aqueous solution. *Environ. Sci. Pollut. Res.* **24** (4), 4200–4209.

Sen, T. K., Afroze, S. & Ang, H. M. 2011 Equilibrium, kinetics and mechanism of removal of methylene blue from aqueous solution by adsorption onto pine cone biomass of Pinus radiata. *Water Air Soil Poll.* **218** (1–4), 499–515.

Song, C., Shan, S., Müller, K., Wu, S., Niazi, N. K., Xu, S., Shen, Y., Rinklebe, J., Liu, D. & Wang, H. 2017 Characterization of pig manure-derived hydrochars for their potential application as fertilizer. *Environ. Sci. Pollut. Res.* **2**, 1–8.

Srivastava, S., Gupta, V. & Mohan, D. 1997 Removal of lead and chromium by activated slag-A blast-furnace waste. *J. Environ. Eng.* **123** (5), 461–468.

Tian, Z., Yang, B., Cui, G., Zhang, L., Guo, Y. & Yan, S. 2014 Synthesis of poly(m-phenylenediamine)/iron oxide/acid oxidized multi-wall carbon nanotubes for removal of hexavalent chromium. *RSC Adv.* **5** (3), 2266–2275.

Vakili, M., Rafatullah, M., Salamatinia, B., Abdullah, A. Z., Ibrahim, M. H., Tan, K. B., Gholami, Z. & Amouzgar, P. 2014

Application of chitosan and its derivatives as adsorbents for dye removal from water and wastewater: a review. *Carbohydr. Polym.* **113**, 115–130.

Xu, Q., Qian, Q., Que, A., Ai, N., Zeng, G. & Wang, J. 2013 Hydrothermal carbonization of macroalgae and the effects of experimental parameters on the properties of hydrochars. *Acs Sustain. Chem. Eng.* **1** (9), 1092–1101.

Yuan, X., Leng, L., Huang, H., Chen, X., Wang, H., Xiao, Z., Zhai, Y., Chen, H. & Zeng, G. 2015 Speciation and environmental risk assessment of heavy metal in bio-oil from liquefaction/pyrolysis of sewage sludge. *Chemosphere* **120**, 645–652.

Zhang, H., Zhang, F. & Huang, Q. 2017 Highly effective removal of malachite green from aqueous solution by hydrochar derived from phycocyanin-extracted algal bloom residues through hydrothermal carbonization. *RSC Adv.* **7**, 5790–5799.

Zhen, G., Lu, X., Li, Y. & Zhao, Y. 2014 Combined electrical-alkali pretreatment to increase the anaerobic hydrolysis rate of waste activated sludge during anaerobic digestion. *Appl. Energ.* **128** (3), 93–102.

First received 8 March 2018; accepted in revised form 14 August 2018. Available online 23 August 2018